

This is an Open Access document downloaded from ORCA, Cardiff University's institutional repository:<https://orca.cardiff.ac.uk/id/eprint/145739/>

This is the author's version of a work that was submitted to / accepted for publication.

Citation for final published version:

Kul, Seda, Anayi, Fatih and Meydan, Turgut 2022. Experimental comparison of localised magnetostriction difference under sinusoidal and PWM excitations. *Journal of Magnetism and Magnetic Materials* 544 , 168692. 10.1016/j.jmmm.2021.168692

Publishers page: <http://dx.doi.org/10.1016/j.jmmm.2021.168692>

Please note:

Changes made as a result of publishing processes such as copy-editing, formatting and page numbers may not be reflected in this version. For the definitive version of this publication, please refer to the published source. You are advised to consult the publisher's version if you wish to cite this paper.

This version is being made available in accordance with publisher policies. See <http://orca.cf.ac.uk/policies.html> for usage policies. Copyright and moral rights for publications made available in ORCA are retained by the copyright holders.



42 important that vibration and noise characterizations of power transformers are determined and considered during
43 the manufacturing stage in industry. Increasing non-linear loads over time affect the aging and lifetime of
44 transformers. Such cases also cause to change the nominal values of transformers. It is important that mechanical
45 parameters such as vibration and noise can be accurately measured and examined so that all necessary functions
46 can be entirely performed as other electromagnetic performances. For this reason, it is necessary to analyze the
47 vibration movements of transformer cores and determine their characteristics, especially locally under changing
48 operating conditions [1]. The noise and vibration causes of the transformer are varied and are mentioned in [2].
49 Although it is generally known that they are caused by magnetostriction and electromagnetic forces, it also depends
50 on magnetostrictive properties of the magnetic core material, the design of corner joints, and the stacked type of
51 core lamination [3]. When the magnetic flux transfers to cross-over materials, especially in the core joints, even
52 localized small movement, the electromagnetic force causes noise and vibration. Moreover, according to [4],
53 magnetostriction depends on clamping, flux density distribution, magnetic properties of electrical steel behavior,
54 deformation of core laminations, etc. Thus it is known as a no-load noise of the core and is generally determined
55 experimentally.

56 Magnetostriction changes the lamination dimension of the material in response to the magnetization of the core
57 [5]. The critical problem in the overall design of the transformer is that the core material has higher
58 magnetostriction and noise based on stacking and joint types, especially in the inter-layers of the core. In addition,
59 the applied voltage type is another affecting factor in this situation. Therefore, many techniques have been applied
60 to determine the magnetic characterization of the core and its dependent variables. Studies have incorporated
61 various measurement methods, sensor techniques, analyses, and experimental research related to the computation
62 and evaluation of magnetostriction. Also, realistic solutions can be obtained by using the Finite Element Method
63 (FEA) to determine magnetic flux density and losses due to the non-linear characteristic of the core. 3D electrical
64 and electromagnetic analyzes can be done on time dependency by using FEA.

65 The first issue that this study will focus on is the measurement technique used during the experimental study. There
66 are various methods to measure magnetostriction, such as optical methods, laser vibrations, strain gauges.
67 Although strain gauges are the oldest and most common, their sensitivity is limited [6]. However, laser and optical
68 methods have higher sensitivity than strain gauges. Despite this, It is preferred in the measurements to be made
69 in the localized and inter-laminations in terms of ease of use and not being affected by temperature. [4,7–9].

70 Another issue is the excitation voltage applied during the operation. Studies carried out so far have generally been
71 conducted using sinusoidal voltage [4,9–14]. These studies are only cover works where measurements are made
72 using strain gauges. In the analyzes made with different voltage types, harmonic components were used in addition
73 to the sine and their comparisons were made.

74 In [13,15,16], researchers examined the harmonic components effect and compared the overall magnetostriction
75 measurement using single sheet samples with different methods. Then [5,17] used PWM excitation and studied
76 harmonic and switching frequency effects to show caused higher magnetostriction. Even if they use PWM
77 excitation, it is just for overall measurement or localized magnetostriction measured on the surface of the core.

78 Our motivation is that localised strain values were measured and compared for different core locations with the help
79 of strain gauges all fixed on top and bottom of test laminations under PWM and sinusoidal excitation voltages. As
80 mentioned [3,18–20], the air gap and joint types affect the magnetostriction considerably. Since the magnetic flux
81 density and strength are higher in the core joints, these regions were considered for localized strain measurements.
82 The results of the experiment were evaluated by considering the studies in the literature. Thus, we contribute to a

83 better understanding of the effect of measured localised strain values on PWM excitation voltage compared to sine
84 excitation voltage.

85 In this study, to validate the accuracy of the experimental method in this article, a no-load strain measurement was
86 performed on a real three-phase dry-type transformer in the laboratory. Localized magnetostriction in the rolling
87 and transverse directions of the upper and lower sides of the lamination under sinusoidal and PWM excitation was
88 measured, analyzed, and compared with each other in terms of the location of the sensors. It does not include
89 frequency dependence, especially under PWM stimulation; only 800 Hz switching frequency was used. The
90 fundamental frequency was 50 Hz, similar to the sinusoidal excitation frequency. ANSYS/Maxwell was used to
91 show the magnetic flux density and force distribution, especially in the middle limb and at joints. It is modeled
92 and analyzed under no-load conditions. The instantaneous values and images obtained from these time dependant
93 analyses help us to better interpret the magnetostriction values according to the regions.

94 It is possible to summarise the main purpose of this study as follows:

95 - To measure the strain value between localized inter-laminations by strain gauge method under sinusoidal and
96 PWM simulations.

97 - Comparing results for accuracy and performance using characteristic measurements at different positions on the
98 top and bottom of the same lamination.

99 - Analysis of transformer core to show magnetic flux density and force via FEA at different excitation values.

100
101 The rest of the paper is organized as follows. Section 2 describes the materials and methods. Experimental
102 setup and measurements have been explained in section 3. Results and discussions are shown in section 4. The
103 conclusions are summarised in section 5.

104

105 2. MATERIALS AND METHODS

106

107 2.1 Strain Gauge Method

108

109 There are several methods to measure magnetostriction in electric machines. Optical methods are trendy;
110 however, the strain gauge method has been used mainly for localized measurement. This method has some
111 disadvantages; careful measures should be taken in fitting strain gauges since the lamination coating has to be
112 removed completely. The strain gauges also have a limited fatigue time.

113 Pro wire foil strain gauge is shown in Fig. 1. It consists of a thin film attached to the probe wires. The
114 electrical resistance of the wire varies in proportion to the amount of strain it experiences.

115



116

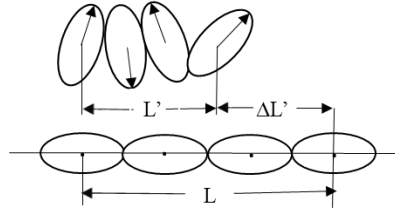
117

Figure 1. Pro wire foil strain gauge.

118 2.2 Magnetic Flux Density and Magnetostriction Under Sinusoidal and Rectangular Waveforms

119

120 Magnetostriction is defined as changing in dimension when the material is subjected to the magnetic field.
 121 The measured strain result is called magnetostriction [20].
 122



123
 124 **Figure 2.** Magnetostriction schematic diagram [20].

125 From the magnetostriction definition, there is a relation between excitation voltage, flux density, and
 126 magnetostriction. It is seen in the following equations for sinusoidal excitation [21,22]:
 127

128
$$U_0 \sin \omega t = -N_1 A \frac{dB}{dt} \quad (1)$$

129
 130
$$B = \frac{-U_0}{N_1 A} \int \sin \omega t = \frac{U_0}{N_1 A} \cos \omega t = B_m \cos \omega t \quad (2)$$

131
 132
 133 B , N_1 , A , μ , B_m are called magnetic flux density, the number of turns, cross-sectional area, the magnetic
 134 permeability of the core, and the peak magnetic flux density, respectively.

135 The relation between magnetic flux density and voltage for rectangular waveform excitation is as follow
 136 [23]:

137
$$u(t) = -N_1 A \frac{dB(t)}{dt} \quad (3)$$

138
 139
$$\int_0^T \left| \frac{dB(t)}{dt} \right|^k dt = \frac{1}{(N_1 A)^k} \int_0^T |u(t)|^k dt \quad (4)$$

140
 141 k is constant in derivation. The solution function of the rectangular waveform in one cycle is:
 142

143
$$u(t) = U_m \begin{cases} 0 & 0 < t < T(1-D)/2 \\ 1 & T(1-D)/2 < t < T/2 \\ 0 & T/2 < t < T(2-D)/2 \\ -1 & T(2-D)/2 < t < T \end{cases} \quad (5)$$

144
 145
$$U_{rms} = Kf B_m A \quad (6)$$

146
 147 K , the transformer excitation voltage form factor is selected as 1 for rectangular wave excitation and 1.11
 148 for sinusoidal excitation [24].

149 Because of the voltage excitation waveform, magnetic flux density behavior also has a linear behavior [23]:
 150
 151

$$152 \quad B(t) = B_m \begin{cases} -1 & 0 < t < T(1-D)/2 \\ -1 + \frac{4}{TD} \left[t - \frac{T(1-D)}{2} \right] & T(1-D)/2 < t < T/2 \\ 1 & T/2 < t < T(2-D)/2 \\ -1 + \frac{4}{TD} \left[t - \frac{T(2-D)}{2} \right] & T(2-D)/2 < t < T \end{cases} \quad (7)$$

$$153 \quad B_m = \frac{U_m D}{4N_1 A f} \quad (8)$$

154
 155 Using magnetic flux density and flux density derivations, from Eqn (1) to Eqn (8), magnetostriction
 156 coefficient (λ) can be derived in Eqn (9) [21,22].
 157

$$158 \quad \lambda = \frac{\Delta l}{l} = \frac{\epsilon_s U_0^2}{(N_1 \omega A B_s)^2} \cos^2 \omega t \quad (9)$$

159
 160 ϵ_s is the coefficient of magnetostriction saturation.
 161 According to Eqn. (9), there is a direct relation between strain value, excitation voltage level, and magnetic
 162 flux density. Significantly for localized measurement, this relation is beneficial to estimate the strain value by
 163 finding the magnetic flux density.
 164 In addition, according to Eqn. (9), the magnetostriction coefficient varies according to the amplitude of
 165 excitation voltage. Therefore, magnetostriction occurs with a fundamental frequency of 100 Hz for an excitation
 166 voltage of a fundamental frequency of 50 Hz.
 167

168 3. Experimental Set-up and FEA Analysis of 3-Phase Dry-Type Transformer

169 A three limb three-phase transformer core was built from 264 layers, a single-step lap, three laminations
 170 per step layer of 0.3mm grain-oriented silicon electrical steel. For sinusoidal excitation, the transformer core was
 171 energized through three-phase variacs for voltage regulations. An inverter (Parker AC10 IP20 5.5kW 400V 3ph
 172 AC Inverter Drive) was used to supply PWM excitation power to the three primary windings of the core and
 173 allowed the core to be magnetized at peak flux density from 0.5T to 1T. The primary and secondary windings,
 174 both connected in star configurations, had 50 turns each. For each setting, the fundamental frequency is 50 Hz.
 175 Switching frequency and modulation index are two essential parameters in PWM applications, therefore switching
 176 frequency was chosen as 800 Hz. The output voltage was adjusted by changing the modulation index under the
 177 PWM excitation.

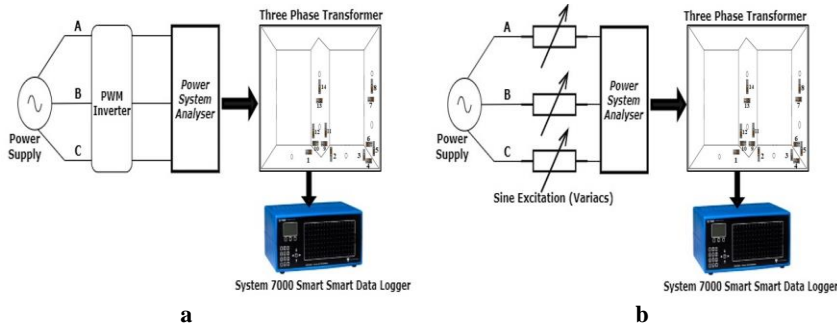
178 The diagrams represent the experimental setup of the three-phase transformer under sinusoidal and PWM
 179 excitations under no-load operation are shown in Fig. 3 (a) and (b), where the strain gauge positions in the core
 180 are illustrated. In order to measure the strain value, strain gauge sensors were used.
 181
 182

183 Table 1 shows the specification of the strain gauge data logger used to collect the strain values at different
 184 transformer core locations simultaneously.

185
 186 **Table I.** Specification of StrainSmart® Data Acquisition System/ Vishay System 7000 Strain Smart Data
 187 system [25].

Measurement accuracy	±0.05%
Measurement resolution	0.5 µstrain
Gauge factor	2
Scan rate per second	2048
Chanel number	Up to 128
Bridge resistor	120

188
 189
 190 Strain gauge specifications are shown in Table II. The lamination coating where the strain gauges adhered
 191 to was removed entirely to directly make good contact with the steel. Then strain gauge arrays were connected to
 192 the data acquisition card via twisted wires to avoid detecting any harmonic noise from the surroundings. The
 193 laminations were stacked and clamped with the torque wrench at 5 Nm.



194 **Figure 3.** Experimental setup for a) PWM excitation b) sinusoidal excitation.

195
 196 **Table II.** Strain gauge specifications.

Features	Value
Gauge Length	8mm
Gauge Factor	2
Gauge Resistance	120Ω
Length	13mm
Width	4mm
Minimum Operating Temperature	-30°C
Maximum Operating Temperature	+180°C
Dimensions	13 x 4 mm

197
198
199
200
201
202
203
204
205
206

The strain data of the core lamination were acquired and saved through the data logger software. For all different magnetic flux density situations, measurements were repeated three times and averaged to minimize undesirable changes in sensor detection sensitivity. The saved numerical data were analyzed using LabVIEW and MATLAB software.

On both sides of the transformer test lamination, twenty-eight strain gauges have been attached at predefined locations (see Fig. 4). Measurements were repeated for three different magnetic flux density conditions: 0.5T, 0.8T, and 1T. Therefore, a reference single-turn search coil was used in the middle limb of the transformer to calculate flux density between A and B points, as shown in Fig. 4.b.

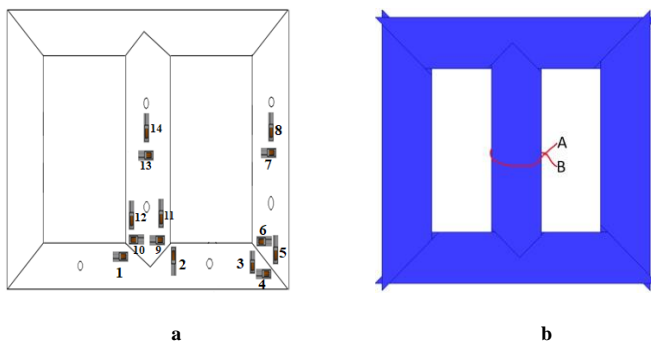


Figure 4. a) The location of the strain gauges in the lamination **b)** Reference search coil position.

207
208
209
210
211
212
213
214
215
216
217
218
219
220

Each strain value on the top and bottom sides of the lamination was measured to compare each other for the sinusoidal and PWM excitations. The measured strain values on the top and bottom sides of the laminations are different. After repeating the measurements three times, the final value is calculated as the mean value of those three measurements. Lamination thickness is an effective parameter for magnetostriction, so these findings are expected since the thickness of the laminations used is 0.3 mm.

In this study, the 3-D FEA model of the three-phase dry-type transformer was modeled using ANSYS/Maxwell software, as shown in the 2D front core shape in Fig. 4.b. Magnetic flux density distribution has been performed with transient analysis to show different magnetic flux density behavior at the same condition and compare practical and simulation results. In addition, the power, loss, and energy distributions in the transformer are seen instantaneously. In this way, the distributions, especially in the joint areas, can be easily seen. Moreover, the line has drawn in the center of the middle limb of the transformer core to obtain the transient magnitude of magnetic flux density, as seen in Fig.5.

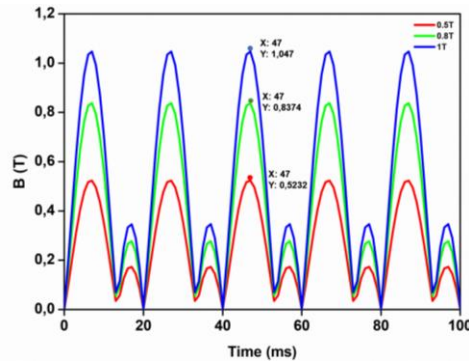


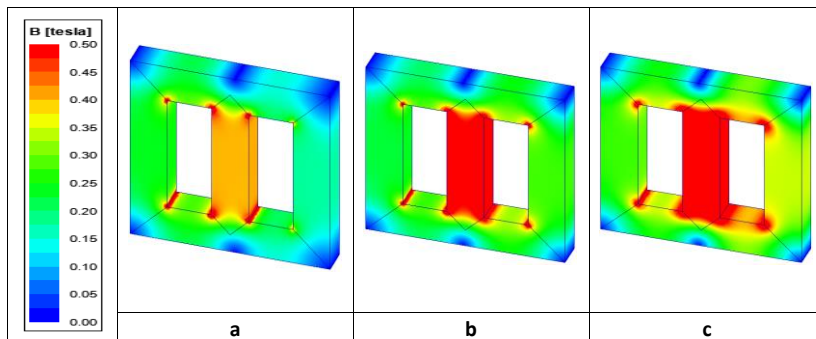
Figure 5. The amplitude of magnetic flux density in the middle limb under sine waveform

4. RESULTS AND DISCUSSIONS

Fig. 4 shows strain gauges localization in the inter-lamination area. Strain gauges were placed intensively in the rolling and transverse directions, especially in the joint areas. There are 14 sensors on both sides of the test lamination. The experiment was carried out using the sine and PWM excitations with a magnetic flux density of 0.5T, 0.8T, and 1T to study the strain across the transformer core under no-load conditions. In this experiment, the clamping factor (5 Nm constant applied torque), lamination thickness, the weight of the stacked lamination on the sensors were fundamental variables for magnetostriction and were kept constant as mechanical stress during the experiment. After experiments were performed, the results were analyzed and compared, as shown in Fig. 6. The results conclude that strain values in PWM simulation are higher than those values under sinusoidal excitation. Moreover, peak to peak strain value increases as expected with higher flux density.

The core laminations were overlapped in one step, so there are overlaps at the corners. Thus, leakages occur between laminations with the effect of air gaps and non-linear flux movements. Therefore, the Maxwell force generates the collision between the laminations to generate magnetostriction. Since it is known that the strain frequency is twice (100 Hz), the fundamental frequency of the excitation voltage a sharper increase in strain and vibration values is expected, especially when PWM excitation is applied.

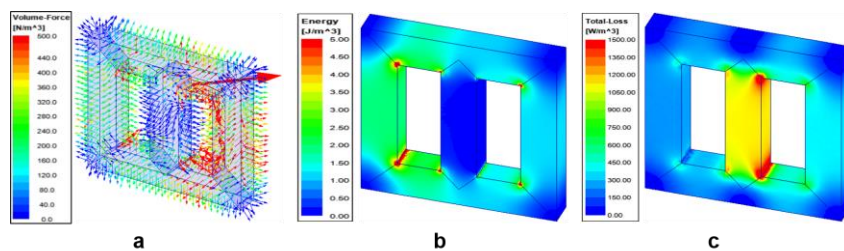
The instantaneous magnetic flux density distributions obtained from time-dependent FEA analyses for 0.5T, 0.8T, and 1T values are shown in Figure 6. All figures were drawn under the same conditions. The maximum value of the localized flux density was 0.5T, approximately as depicted in red color. As can be seen from the figures, when the desired flux density is obtained with the search coil, the flux density in the joint and middle limb is higher than the other parts. These high levels of flux densities have an impact on the distribution of magnetostriction values.



245 **Figure 6.** Magnetic flux density distribution for a) 0.5 T b) 0.8T c)1T.

246 Force, energy, and total loss distributions are instantly shown in Figure 7 under constant magnetic flux density
 247 conditions. As can be seen from the FEA analyses, the densities are again in the joint regions, and all of these
 248 values are the factors that affect the magnetostriction separately. All these analysis results support each other, thus
 249 considering the non-linear behavior of the transformer, the importance of local consideration of experimental
 250 measurements and evaluations becomes apparent. This situation is also important to carry out and evaluate the
 251 experiments locally, especially highlighting the issues that magnetostriction should be considered at the design
 252 stage.

253



254 **Figure 7. a)** Force distribution **b)** Energy distribution **c)** Total loss distribution for same magnetic flux density
 255 condition.
 256

257 Six positions have been chosen for discussion, 2 of them in transverse directions the others in rolling directions;
 258 these are numbered as 3, 9 and 1, 5, 8, 14 strain gauges, respectively. It is expected that the strain value in the
 259 transverse direction is lower than in rolling directions. However, strain values of those locations in the corner are
 260 also expected to be higher. Due to the higher magnetic flux density at the joint region, the strain values in the
 261 transverse direction are as high as the rolling ones.

262 Fig. 8 shows the measured peak to peak strain values of the sensors mentioned above. The graphs show four
 263 different values for each magnetic flux density of 0.5T, 0.8T, and 1T. The four different values represent outputs
 264 of sensors attached to the top and bottom of the test lamination at the same locations under sinusoidal and PWM
 265 excitations.

266 It can be seen from Figure 8 that there is a consistency in the variations of strain values at the top and bottom of
267 the test lamination. This is illustrated as reducing stress values under the test laminations on the lower yoke
268 (Sensors 1 and 3). Similar behavior has been noticed for the two sensors located at the middle of the central and
269 outer limbs (Sensors 8 and 14) near the clamping locations. The opposite behavior on the central and outer limbs
270 near the joints (Sensors 5 and 9) is also depicted in this figure. These trends are applicable to the three excitations
271 at 0.5T, 0.8T, and 1T, all under sinusoidal and PWM energizations.

272 The variations of the strain values on the top and bottom of the test lamination are attributed to the lamination
273 bending effect at different locations across the transformer core. The bending might be originated from the
274 roughness of the lamination surfaces and the locations of the bolts that secure the laminations together. This study
275 provides the best locations for the bolts to achieve the lowest value of generated noise due to the magnetostriction.

276 Sensors 3 and 9 are in the transverse direction. Therefore, it is expected to have a lower strain than the other four
277 sensors; however, they are close to the joint areas. Therefore, the values measured with these two sensors are
278 almost equal to the values of other sensors.

279 Although sensor 5 in rotational position does not seem close to the joint region, the strain value is larger than the
280 others in the PWM excitation condition due to overlaps vibrations.

281 These findings show that each strain gauge has its magnetostriction value. Moreover, magnetostriction is affected
282 by the local variables due to the area where the sensor is attached.

283 Each of these values is at a fundamental frequency. As we mentioned in the reference work above [8,9,22], it is
284 seen that the strain values in the PWM excitation state are much higher than in the sinusoidal excitation state. The
285 most important point to be considered is that to accommodate sensors above and below same points on the test
286 lamination, air gaps are created in the transformer core in the inter-lamination regions. The weights of all
287 laminations on the sensor are also effective. The transformer is tested laid in a horizontal position. In addition,
288 since strain gauges are very sensitive to external sounds, 25-44 ppm peak values are acceptable, especially in PWM
289 excitations.

290 In sinusoidal wave excitation, the voltage varies from 0 to max or min value as a wave, but in PWM, it only
291 progresses as min and max excitation voltage. In this case, the values in the graph explain the rise of the strain
292 values in the PWM state up to approximately two times for the 0.8T and 1T excitations.

293

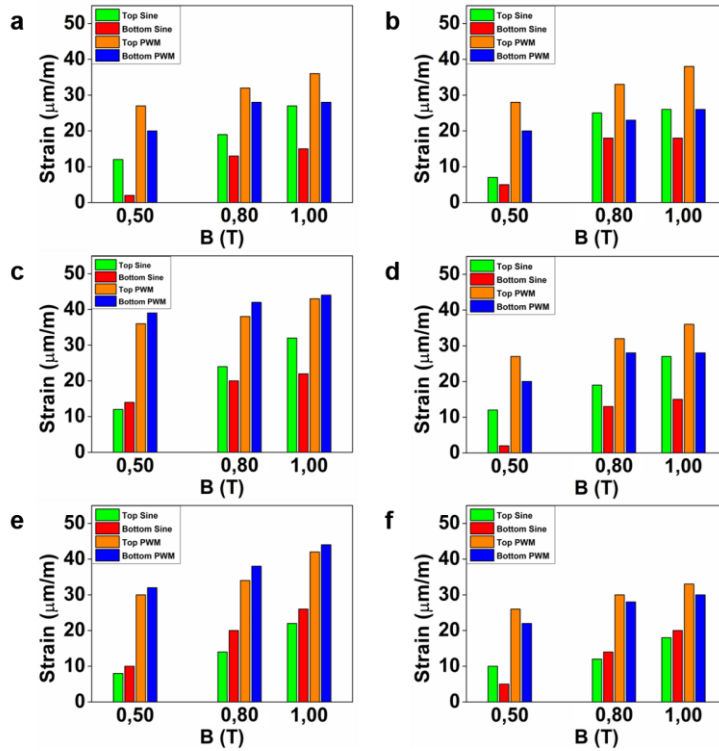


Figure 6. Localized peak to peak strain value at different flux densities on both sides of the lamination under sine and PWM excitations a) sensor 1 b) sensor 3 c) sensor 5 d) sensor 8 e) sensor 9 f) sensor 14.

In sinusoidal wave excitation, the voltage varies from 0 to max or min value as a wave, but in PWM, it only progresses as min and max excitation voltage. In this case, the values in the graph explain the rise of the strain values in the PWM state up to approximately 2 times for the 0.8T and 1T excitations.

5. CONCLUSIONS

This study intends to show the differences in strain values at localized interlaminar positions for the no-load condition under two different excitation voltages. All the measurements are subject to different magnetic flux densities, and transient finite element analysis of magnetic flux distribution in the core was conducted. The following results were obtained as follows:

- Since inter-lamination was studied, higher magnetostriction values were obtained than other studies, even under sinusoidal excitation.

- Since excitation occurs with peak values as max and min, strain values in PWM excitation are quite high compared to sinusoidal excitation.

- Since the magnetic flux density, loss distribution and forces are higher at the joint regions, high strain values are obtained from the sensors close to those regions, even if they are in the transverse direction. Since the magnetic

Formatted: Not Highlight

314 flux density is higher at the joint regions, high strain values are obtained from the sensors close to those regions,
315 even if they are in the transverse direction.

316 - PWM excitation is used at a fixed 800 Hz switching frequency. Therefore, the comparison was made only as
317 sinusoidal and PWM excitations according to the lower and upper sensor values.

318 - Even if the measurement is taken from the same point, different values are read from the sensors located above
319 and below the test lamination. This is due to the effect of the air gap, lamination thickness, and external sounds.

320 Future studies aim to examine and show the magnetostriction differences under PWM excitation at various
321 switching frequencies.

322

323 Acknowledgments

324

325 This study is partially supported by the Wolfson Center for Magnetism at Cardiff University.

326 One of the authors (SK) was sponsored by the Higher Education Council of Turkey.

327

328 References

329 [1] F. BATTAL, I. SEFA, S. BALCI, Doğrusal Olmayan Yük Koşullarında Çalışan Kuru Tip
330 Transformatörlerin Titreşim Etkileri Üzerine Bir Analiz, Gazi Üniversitesi Fen Bilim. Derg. Part C
331 Tasarım ve Teknol. 7 (2019) 729–740. <https://doi.org/10.29109/gujsc.580521>.

332 [2] L. Lahn, C. Wang, A. Allwardt, T. Belgrand, J. Blaszkowski, Improved transformer noise behavior by
333 optimized laser domain refinement at thyssenkrupp electrical steel, in: IEEE Trans. Magn., 2012: pp.
334 1453–1456. <https://doi.org/10.1109/TMAG.2011.2173924>.

335 [3] A.J. Moses, P.I. Anderson, T. Phophongvivat, Localized Surface Vibration and Acoustic Noise Emitted
336 from Laboratory-Scale Transformer Cores Assembled from Grain-Oriented Electrical Steel, IEEE Trans.
337 Magn. 52 (2016). <https://doi.org/10.1109/TMAG.2016.2584004>.

338 [4] G. Shilyashki, H. Pfütznern, P. Hamberger, M. Aigner, A. Kenov, I. Matkovic, Spatial distributions of
339 magnetostriction, displacements and noise generation of model transformer cores, Int. J. Mech. Sci. 118
340 (2016) 188–194. <https://doi.org/10.1016/j.ijmecsci.2016.09.022>.

341 [5] S. Somkun, A.J. Moses, P.I. Anderson, Mechanical resonance in nonoriented electrical steels induced by
342 magnetostriction under PWM voltage excitation, in: IEEE Trans. Magn., 2008: pp. 4062–4065.
343 <https://doi.org/10.1109/TMAG.2008.2001585>.

344 [6] N.B. Ekreem, A.G. Olabi, T. Prescott, A. Rafferty, M.S.J. Hashmi, An overview of magnetostriction, its
345 use and methods to measure these properties, J. Mater. Process. Technol. 191 (2007) 96–101.
346 <https://doi.org/10.1016/j.jmatprotec.2007.03.064>.

347 [7] Y. Kai, Y. Tsuchida, T. Todaka, M. Enokizono, Measurement of the two-dimensional magnetostriction
348 and the vector magnetic property for a non-oriented electrical steel sheet under stress, in: J. Appl. Phys.,
349 2012. <https://doi.org/10.1063/1.3673807>.

- 350 [8] G. Shilyashki, H. Pftzner, J. Anger, K. Gramm, F. Hofbauer, V. Galabov, E. Mulasalihovic,
351 Magnetostriction of transformer core steel considering rotational magnetization, *IEEE Trans. Magn.* 50
352 (2014) 1–40. <https://doi.org/10.1109/TMAG.2013.2283193>.
- 353 [9] C.C. Linhares, J.E. Santo, R.R. Teixeira, C.P. Coutinho, S.M.O. Tavares, M. Pinto, J.S. Costa, H. Mendes,
354 C.S. Monteiro, A. V. Rodrigues, O. Frazão, Magnetostriction assessment with strain gauges and fiber
355 bragg gratings, *EAI Endorsed Trans. Energy Web.* 7 (2020) 1–9. [https://doi.org/10.4108/eai.13-7-](https://doi.org/10.4108/eai.13-7-2018.161420)
356 2018.161420.
- 357 [10] T. Hilgert, L. Vandeveld, J. Melkebeek, Comparison of magnetostriction models for use in calculations
358 of vibrations in magnetic cores, *IEEE Trans. Magn.* 44 (2008) 874–877.
359 <https://doi.org/10.1109/TMAG.2007.916395>.
- 360 [11] M. Yamagashira, D. Wakabayashi, M. Enokizono, Vector magnetic properties and 2-D magnetostriction
361 of various electrical steel sheets under rotating flux condition, *IEEE Trans. Magn.* 50 (2014).
362 <https://doi.org/10.1109/TMAG.2013.2290836>.
- 363 [12] A.J. Moses, P.I. Anderson, S. Somkun, Modeling 2-d magnetostriction in nonoriented electrical steels
364 using a simple magnetic domain model, *IEEE Trans. Magn.* 51 (2015).
365 <https://doi.org/10.1109/TMAG.2015.2402111>.
- 366 [13] Y. Zhang, Q. Li, Di. Zhang, B. Bai, D. Xie, C.S. Koh, Magnetostriction of Silicon Steel Sheets under
367 Different Magnetization Conditions, *IEEE Trans. Magn.* 52 (2016) 3–6.
368 <https://doi.org/10.1109/TMAG.2015.2477838>.
- 369 [14] U. Aydin, P. Rasilo, F. Martin, D. Singh, L. Daniel, A. Belahcen, M. Rekik, O. Hubert, R. Kouhia, A.
370 Arkkio, Magneto-mechanical modeling of electrical steel sheets, *J. Magn. Mater.* 439 (2017) 82–
371 90. <https://doi.org/10.1016/j.jmmm.2017.05.008>.
- 372 [15] W. Gong, Z. Zhang, R. Hou, H. Wang, Z. Xu, A. Lin, J. He, W. Fan, J. Wang, Magnetostriction and the
373 Influence of Harmonics in Flux Density in Electrical Steel, *IEEE Trans. Magn.* 51 (2015) 25–28.
374 <https://doi.org/10.1109/TMAG.2015.2440320>.
- 375 [16] P. Anderson, Measurement of the stress sensitivity of magnetostriction in electrical steels under distorted
376 waveform conditions, *J. Magn. Mater.* 320 (2008) 1–6.
377 <https://doi.org/10.1016/j.jmmm.2008.04.014>.
- 378 [17] S. Iida, Y. Okuma, S. Masukawa, S. Miyairi, B.K. Bose, Study on Magnetic Noise Caused by Harmonics
379 in Output Voltages of PWM Inverter, *IEEE Trans. Ind. Electron.* 38 (1991) 180–186.
380 <https://doi.org/10.1109/41.87585>.
- 381 [18] S. Yürekten, Y. Sert, M. Trnan, E. Ceylan, The Parameters of Generated Sound Level of Transformer
382 Cores, *Procedia Eng.* 202 (2017) 273–279. <https://doi.org/10.1016/j.proeng.2017.09.714>.
- 383 [19] H. Shahrouzi, A.J. Moses, P.I. Anderson, G. Li, Z. Hu, Comparison between measured and computed
384 magnetic flux density distribution of simulated transformer core joints assembled from grain-oriented and
385 non-oriented electrical steel, *AIP Adv.* 8 (2018). <https://doi.org/10.1063/1.4994133>.

- 386 [20] D. Jiles, *Introduction to Magnetism and Magnetic Materials*, 2015. <https://doi.org/10.1201/b18948>.
- 387 [21] J. Shengchang, L. Yongfen, L. Yanming, Research on extraction technique of transformer core
388 fundamental frequency vibration based on OLCM, *IEEE Trans. Power Deliv.* 21 (2006) 1981–1988.
389 <https://doi.org/10.1109/TPWRD.2006.876665>.
- 390 [22] M.M. Weiner, Magnetostrictive Offset and Noise in Flux Gate Magnetometers, *IEEE Trans. Magn.* 5
391 (1969) 98–105. <https://doi.org/10.1109/TMAG.1969.1066411>.
- 392 [23] Z. Pengning, L. Lin, Magnetostrictive properties of silicon steel sheet under excitation of different types,
393 *Int. J. Appl. Electromagn. Mech.* 63 (2020) 435–448. <https://doi.org/10.3233/JAE-190146>.
- 394 [24] S. Balci, Thermal behavior of a three phase isolation transformer under load conditions with the finite
395 element analysis, *Therm. Sci.* 24 (2020) 2189–2201. <https://doi.org/10.2298/TSCI190706386B>.
- 396 [25] A. Engineering, H. Ethernet, R. Utility, T. Ethernet, F.I. Response, System 7000 StrainSmart ® Data
397 Acquisition System System 7000, (2012). <http://www.vishaypg.com/docs/11271/system-7000.pdf>.
- 398